



Published in final edited form as:

Mol Pharm. 2009 ; 6(2): 396–406. doi:10.1021/mp800120t.

Effect of modification of the physicochemical properties of ICAM-1-derived peptides on internalization and intracellular distribution in the human leukemic cell line HL-60

Sumit Majumdar^{1,3}, Bimo A. Tejo^{1,4}, Ahmed Badawi¹, David Moore², Jeffrey P. Krise¹, and Teruna J. Siahaan^{1,5}

¹ Department of Pharmaceutical Chemistry, The University of Kansas, Simons Research Laboratories, 2095 Constant Ave., Lawrence, Kansas 66047

² The KU Microscopy and Analytical Imaging Laboratory, The University of Kansas, Lawrence, Kansas 66045

Abstract

The objective of this work is to test the hypothesis that increasing the hydrophilicity of DOX-peptide conjugates may modify their entry mechanisms into HL-60 cells from passive diffusion to receptor-mediated uptake. To test this hypothesis, the entry mechanisms and the intracellular disposition of DOX-cIBR7, DOX-PEGcIBR7, FITC-cIBR, and FITC-cIBR7 were evaluated in HL-60 cells. To increase the hydrophilicity of the peptide, the cIBR peptide (cyclo(1,12)PenPRGGSVLVTGC) was modified to cIBR7 peptide (cyclo(1,8)CPRGGSVC) by removing the hydrophobic residues at the C-terminus. DOX-cIBR7 conjugate, which has higher hydrophilicity than DOX-cIBR, was synthesized. Secondly, a hydrophilic linker (11-amino-3,6,9-trioxaundecanate linker) was incorporated between DOX and cIBR7 to generate DOX-PEGcIBR7 with higher hydrophilicity than DOX-cIBR7. As controls, FITC-cIBR and FITC-cIBR7 were used to check for any endocytic uptake process of the peptide. As previously found with DOX-cIBR, DOX-cIBR7, and DOX-PEGcIBR7, conjugates enter the cells via passive diffusion and not via the energy-dependent endocytic process. This result suggests that an increase in hydrophilicity does not influence the entry mechanism of the DOX-peptide conjugates. In contrast to the DOX-cIBR7 conjugate, the FITC-cIBR7 conjugate showed energy-dependent cellular entry into the cells and followed an endocytic pathway similar to that for dextran. Finally, the entry of DOX-cIBR7 and DOX-PEGcIBR into the cell cytosol was shown to be due to the properties of DOX and not to those of the peptide.

Introduction

Targeted drug delivery methods have been exploited to improve the delivery of cytotoxic drugs in an effort to lower their side effects. These delivery methods normally take advantage of the special features of the target cells compared to other cells in the body. One of these features is the upregulation or selective expression of certain cell surface receptors in many types of cancers compared to normal cells.^{1–3} Furthermore, certain types of cells (leukocytes) express leukocyte function-associated antigen-1 (LFA-1) receptors, which are not expressed in other cell types.^{4,5} Thus, the LFA-1 receptor is an attractive target for improving the delivery of drugs to leukocytes. In general, peptides,⁶ proteins,^{7,8} and antibodies⁹ have been employed

⁵Address correspondence to: Dr. Teruna J. Siahaan, Department of Pharmaceutical Chemistry, The University of Kansas, 2095 Constant Avenue, Lawrence, Kansas 66047, Phone: 785-864-7327, Fax: 785-864-5736, E-mail: E-mail: siahaan@ku.edu.

³Current Address: BD Technologies, 21 Davis Drive, Research Triangle Park, North Carolina 27709

⁴Current Address: Department of Chemistry, Universiti Putra Malaysia, 43400 UPM Serdang, Selangor, Malaysia

as carriers of many cytotoxic drugs to target a specific cell surface receptor with some success in *in vitro* and *in vivo* model systems.

Doxorubicin (DOX), an anticancer agent, has cardiotoxicity as one of its side effects. To lower this side effect, DOX has been conjugated to different carrier molecules such as peptides,¹⁰ proteins¹¹ and other macromolecular carriers.¹² In addition, DOX has fluorescence properties that can be used to follow the distribution of the conjugate in cells and in *in vivo* systems. The cytotoxicity of DOX is due to its intercalation of DNA in the nucleus. DOX structure can be divided into three functional domains: (1) the hydrophobic anthraquinone moiety is for DNA intercalation, (2) several substituents on the cyclohexyl ring are involved in H-bonding with the DNA bases, and (3) the daunosamine sugar moiety can bind to the minor groove of DNA.¹³ DOX has been conjugated to carrier molecules through the primary amine of the daunosamine sugar,¹⁴ C13 ketone functionality,¹⁵ and C14 alcoholic hydroxyl functionality.¹⁰ Among these conjugation sites, the primary amine of the daunosamine sugar moiety has been used to conjugate DOX to many different peptides.^{14,16,17}

Previously, we conjugated DOX to cIBR peptide cyclo(1,12)PenPRGGSVLVTGC to produce DOX-cIBR conjugate.¹⁴ This conjugate entered into the human leukemic cell line, HL-60, in an energy-independent manner (*e.g.*, passive diffusion) and showed a diffuse fluorescence distribution pattern in the cytosol instead of the punctate distribution pattern that was expected for a molecule internalized by receptor-mediated endocytosis.¹⁴ The passive diffusion uptake behavior of DOX-cIBR could be due to its hydrophobicity because the octanol/aqueous buffer distribution ratio (pH 7.4) determination indicated that DOX-cIBR is highly hydrophobic (Log D = 1.15). However, a more hydrophilic fluorescein isothiocyanate- (FITC-) labeled cIBR conjugate (Log D = 0.58) entered the cells via receptor-mediated endocytosis. Although a DOX conjugate with CNGRC cyclic peptide (DOX-CNGRC) for targeting CD-13 receptor shows a distribution similar to DOX-cIBR, the entry of this conjugate has not been fully studied.¹⁰ Therefore, we hypothesize that the hydrophobicity of the conjugate is one of the factors contributing to its passive diffusion rather than the receptor-mediated entry of the conjugate.¹⁴

The present work is designed to test the hypothesis that increasing the hydrophilicity of the conjugates may modify the entry mechanisms of DOX-cIBR-derivatives into HL-60 cells from passive diffusion to receptor-mediated uptake. Two approaches were used to change the physicochemical properties of the conjugate. The first was to alter the hydrophobicity of the peptide by eliminating the hydrophobic residue at the C-terminus of cIBR. In this case, we have modified cIBR peptide to cIBR7 peptide (cyclo(1,8)CPRGG SVC) by eliminating four hydrophobic residues at the C-terminus of cIBR and by replacing the Pen1 residue with a Cys residue (Figure 1).¹⁸ It is interesting to find that cIBR7 peptide has better activity to inhibit heterotypic T-cell adhesion than does the parent cIBR peptide, suggesting that cIBR7 binds more selectively to the I-domain of LFA-1 than does cIBR peptide.¹⁸ The second method was to incorporate an 11-amino-3,6,9-trioxaundecanate linker between DOX and cIBR7 peptide to further increase the hydrophilicity of the conjugate and generate DOX-PEGcIBR7 (Figure 1). Fluorescein isothiocyanate (FITC) was also conjugated to cIBR7 peptide to give FITC-cIBR7; this was used to check for endocytic uptake as was observed for FITC-labeled cIBR (FITC-cIBR).¹⁴ In this work, we compared the entry mechanisms and the intracellular disposition of DOX-cIBR7, DOX-PEGcIBR7, and FITC-cIBR7 in HL-60 cells. The results from these studies allowed us to test whether the changes in the physicochemical properties of the conjugates influenced their entry mechanism.

Experimental Section

Cells and Chemicals

The human acute promyeloid leukemic cell line HL-60 was kindly provided by Dr. Yueshang Zhang (Arizona Cancer Center, University of Arizona). Cells were grown in RPMI 1640 medium supplemented with 10% fetal bovine serum, 100 units/mL of penicillin G sodium, 100 $\mu\text{g}/\text{mL}$ of streptomycin sulfate, and 2.0 g/L of NaHCO_3 . Cells were maintained at a density of 1×10^6 to 2×10^6 cells/mL at 37 °C in a humidified 5% CO_2 atmosphere. Doxorubicin hydrochloride, succinic anhydride, and diisopropylethyl amine were obtained from Sigma Chemicals (St. Louis, MO). Solvents used in peptide synthesis were of pure analytical grade. All reagents, resins, and Fmoc-protected amino acids for peptide syntheses were purchased from Peptides International (Louisville, KY), Advanced ChemTech (Louisville, KY), and Applied Biosystems (Foster City, CA). Fmoc-11-amino-3,6,9-trioxaundecanoic acid (Fmoc-mini-PEG-3TM) was purchased from Peptides International (Louisville, KY) and FITC-dextran (MW 10,000) was from Molecular Probes (Eugene, OR).

Peptide Synthesis

Syntheses of linear IBR7 (CPRGGVC) and PEGIBR7 ($\text{H}_2\text{N}-(\text{CH}_2\text{CH}_2\text{-O})_3\text{-CPRGGVC}$) peptides were performed on a Pioneer peptide synthesizer (PerSeptive Biosystems, CA) using the standard Fmoc solid-phase strategy with O-(7-azabenzotriazole-1-yl)-N,N,N',N'-tetramethyluronium hexafluorophosphate (HATU) as the activating agent. Extended coupling cycles were employed. The resin-containing peptide was washed several times with methylene chloride and then with methanol followed by vacuum drying. A cleavage cocktail containing trifluoroacetic acid (TFA, 90%), 1,2-ethane dithiol (3%), anisole (2%), and thioanisole (5%) was used during peptide cleavage from the solid support followed by precipitation in ice-cold diethyl ether. Diethyl ether solution was allowed to stand overnight at 4 °C for maturation of the precipitate. Subsequently, the peptide precipitate was separated from ether-containing scavengers by centrifugation. The crude linear peptides were purified by semi-preparative C18 reversed-phase HPLC. The cyclization of the linear peptides to give cIBR7 or PEGcIBR7 was carried out by bubbling air overnight into the peptide solution (0.06 mM) containing ammonium bicarbonate (0.05 M) and ammonium hydroxide at pH 8.5. The solution was lyophilized and crude cyclic peptides were purified by semi-preparative C18 reversed-phase HPLC and the fractions were collected every 1.0 mL in a test tube. Each fraction was analyzed by analytical HPLC with analytical C18 column; the fractions containing a single peak of product were pooled and lyophilized. The molecular weights of cIBR7 ($M+1 = 776.3$ amu) and PEGcIBR7 ($M+1 = 965.4$ amu) peptides were confirmed by electrospray ionization mass spectrometry and the purity of these peptides is higher than 96% as determined by analytical HPLC.

Conjugation of Doxorubicin (DOX) with cIBR7 and PEGcIBR7 Peptides

This reaction was performed according to our previously published method.¹⁴ Briefly, the amino group in the sugar moiety of DOX was reacted with succinic anhydride in dimethyl formamide (DMF) in the presence of diisopropylethyl amine to give DOX-succinate ($M+1 = 643$ amu) (Figure 2). Subsequently, DOX-succinate was reacted with the N-terminus of cIBR7 or PEGcIBR7 in the presence of HBTU (O-benzotriazole-N,N,N',N'-tetramethyl-uronium-hexafluoro-phosphate) in DMF to give DOX-cIBR7 or DOX-PEGcIBR7, respectively (Figure 2). The progress of the reaction was monitored with C18 reversed-phase analytical HPLC. Both of the DOX-conjugates were purified using semi-preparative HPLC with a C18 column. The fractions were collected every 1.0 mL in a test tube. Each fraction was analyzed by analytical HPLC with analytical C18 column. The fractions with a pure product (a single peak) were combined and lyophilized. The identity of each product was confirmed by mass spectrometry with $M+1 = 1401.5$ amu for DOX-cIBR7 and $M+1 = 1590.6$ amu for DOX-PEGcIBR7.

Conjugation of FITC with cIBR7 and cIBR Peptides

Conjugation of FITC with cIBR7 was done according to our previously published method.^{14,19} Briefly, pure cIBR7 peptide (0.06 mmol) was dissolved in 5 mL of Nanopure water; 0.12 mmol fluorescein-5-isothiocyanate (Sigma) was added to the peptide solution, and the pH was adjusted to 10 by addition of 1.0 N NaOH solution. After stirring for 2 h with a magnetic stirrer, the reaction mixture was neutralized by the addition of 10% v/v acetic acid solution. The solution was lyophilized and the resulting crude product of FITC-cIBR7 was purified by semi-preparative C18 reversed-phase HPLC. The pure FITC-cIBR7 was analyzed by analytical C18 reversed-phase HPLC and identified by electrospray ionization mass spectrometry ($M+1 = 1165.3$). Conjugation of FITC with cIBR was done in an identical manner and is described elsewhere.¹⁴

Determination of Octanol/Aqueous Buffer Distribution Ratios (pH 7.4) for DOX-cIBR7 and DOX-PEGcIBR7 Conjugates

1.0 mL of *n*-octanol (Fisher) was added to 10 mL of phosphate-buffered saline (PBS) (pH 7.4) containing 2.0 μM of DOX-cIBR7 or DOX-PEGcIBR7 in a separatory funnel and was mixed for 30 min. The two phases were allowed to equilibrate for 24 h while protected from light. The concentration of DOX-cIBR7 or DOX-PEGcIBR7 in each phase was determined using a fluorescence spectrophotometer (RF5000U, Shimadzu Inc., Kyoto, Japan). The fluorescence intensity of DOX-cIBR7 or DOX-PEGcIBR7 in aqueous buffer solutions (pH 7.4) was measured at different concentrations, and individual calibration curves were generated using Microcal Origin version 6.0.

Temperature-dependent Internalization Studies of DOX-cIBR7, DOX-PEGcIBR7, and DOX using HL-60 Cells

HL-60 cells were centrifuged and resuspended in RPMI 1640 medium at a concentration of 2×10^6 cells/mL. 250 μL of the cell suspension was added separately to 250 μL of a solution of DOX-cIBR7, DOX-PEGcIBR7, and DOX to reach a final conjugate or drug concentration of 10 μM . Cell viability during incubation at this concentration of the compounds was confirmed separately using Trypan Blue staining (data not shown). The cells were incubated at 37 °C and 4 °C for 1 h while protected from light, and then centrifuged at 1000 rpm for 2 min. The cells were washed three times with ice-cold PBS and suspended in 20 μL of PBS. Final cell density used for the microscopic observation was 25×10^6 cells/mL. 10 μL of the cell suspension in PBS was put on a slide for observation. A Nikon Eclipse 80i microscope equipped for epifluorescence was used to view the cells, and the fluorescence emissions of DOX were observed using a rhodamine filter set. Untreated cells were viewed with the same filter to check for autofluorescence. The images were captured using an Orca ER camera (Hamamatsu, Inc., Bridgewater, NJ) controlled by the Metamorph program (Version 6.2, Universal Imaging Corp., West Chester, PA).

Temperature-dependent Internalization Studies of FITC-cIBR7 using HL-60 Cells

HL-60 cells were incubated in PBS at a cell density of 5×10^5 cells/mL for 10 min at 37 °C and resuspended in PBS at a cell density of 2×10^6 cells/mL. 250 μL of cell suspension was added separately to 250 μL of FITC-cIBR7 (125 μM , in PBS) and 250 μL of FITC-dextran (200 μM , in PBS). Cells were incubated at 37 °C and at 4 °C in the dark for 1 h. After the incubation, cells were treated as described above. Control cells without any compound were treated and prepared in the same manner. Cells were observed using a CSU-10 Yokogawa-type spinning disk confocal microscope, a 473 nm diode-pumped solid state (DPSS) laser for fluorophore excitation, and an emission filter at 525 ± 15 nm. Images were captured using a $1\text{K} \times 1\text{K}$ EM-CCD camera (Hamamatsu) controlled by the SlideBook image capture program (version 4.1, Intelligent Imaging Innovations, Denver, CO).

Colocalization Studies of FITC-cIBR and FITC-cIBR7 with Alexa 647-Dextran using HL-60 Cells

For the colocalization studies, HL-60 cells were washed with PBS and resuspended in PBS at a cell density of 2×10^6 cells/mL. 5×10^5 cells were incubated with $25 \mu\text{M}$ Alexa 647-conjugated dextran (dextran, Alexa Fluor® 647; 10,000 MW, anionic, fixable; Molecular Probes®, Eugene, OR) and $125 \mu\text{M}$ FITC-cIBR or FITC-cIBR7 for 1 h at 37°C . At the end of the incubation, cells were washed three times with ice-cold PBS and finally resuspended in $20 \mu\text{L}$ of PBS. $10 \mu\text{L}$ of the cell suspension in PBS was placed on a slide for microscopic observation. Untreated cells were also viewed under the same conditions to check for autofluorescence. Cells were visualized using either the 473 nm or 653 nm DPSS laser line of the spinning disk confocal microscope for excitation, with detection performed using either the 525 ± 15 nm or the 660 long-pass emission filter where appropriate. Images were captured using an EM-CCD camera (Hamamatsu) controlled by the SlideBook program (version 4.1).

Results

Syntheses of DOX-cIBR7, DOX-PEGcIBR7, FITC-cIBR7, and FITC-cIBR

The linear peptides IBR7 and PEGIBR7 were synthesized by the solid-phase method using Fmoc chemistry and were purified by semi-preparative HPLC. Both linear peptides were cyclized by air oxidation in high dilution conditions to give cIBR7 and PEGcIBR7. Then, cIBR7 and PEGcIBR7 cyclic peptides were conjugated to DOX-succinate to yield DOX-cIBR7 and DOX-PEGcIBR7 (Figure 2). FITC-cIBR7 and FITC-cIBR were also synthesized and purified using semi-preparative HPLC.

Determination of Octanol/Aqueous Buffer Distribution Ratios (pH 7.4) for DOX-cIBR7 and DOX-PEGcIBR7 Conjugates

The results from the octanol/aqueous buffer distribution ratio studies are presented in Table 1. It is clear that the DOX-cIBR7 conjugate is more hydrophilic (distribution ratio = 4.3, pH 7.4) than DOX-cIBR (distribution ratio = 14.1, pH 7.4),¹⁴ indicating that removal of the C-terminal hydrophobic amino acid residues (*i.e.*, LVTG) had a significant effect on the physicochemical properties of the conjugate. As expected, incorporating a hydrophilic linker into DOX-PEGcIBR7 further enhanced its hydrophilicity to a distribution ratio of 0.9 at pH 7.4 (Table 1). Therefore, changes in the structures of the conjugates alter their physicochemical properties from a high hydrophobic DOX-cIBR to a hydrophilic DOX-PEGcIBR7 conjugate.

Temperature-dependent Internalization of DOX-cIBR7 and DOX-PEGcIBR7 in Comparison to DOX using HL-60 Cells

Because the receptor-mediated entry processes are energy dependent, reduction of temperature suppresses the endocytic uptake pathway. Therefore, the internalization mechanisms of DOX-cIBR7, DOX-PEGcIBR7, and DOX were evaluated at 37°C and 4°C . Both DOX-cIBR7 (Figure 3) and DOX-PEGcIBR7 (Figure 4) conjugates showed a diffuse fluorescence distribution pattern in the cellular cytoplasm at 37°C (Figures 3a and 4a). There were no punctate endocytic fluorescence localization patterns inside the cells. A similar fluorescence pattern was seen for DOX-cIBR.¹⁴ The internalization of DOX-cIBR7 and DOX-PEGcIBR7 conjugates at 4°C produced a diffuse fluorescence of the conjugates inside the cell cytosol (Figures 3b and 4b) without any apparent difference from the internalization at 37°C . These results suggest that the entry of DOX-cIBR7 and DOX-PEGcIBR7 conjugates was not via an endocytic pathway but via passive diffusion. As observed previously, DOX itself was localized inside the nucleus when incubated at 37°C with the cells for 1 h (Figures 3c and 4c). Lowering the temperature to 4°C reduced the fluorescence intensity of DOX, indicating that the uptake of DOX was suppressed and the distribution was no longer completely localized in the cell

nucleus (Figures 3d and 4d). Instead, DOX was distributed throughout the cell, including the cell cytoplasm as described previously.¹⁴ Temperature-dependent entry of DOX has been proposed to be due to the aggregation of DOX molecules.²⁰ Increasing the hydrophilicity of the conjugates did not change the mode of entry of DOX-cIBR7 and DOX-PEGcIBR7 conjugates from passive diffusion to receptor-mediated endocytosis. It is possible that the DOX portion of the conjugate has more impact on the uptake behavior than does the peptide fragment.

Temperature-dependent Internalization of FITC-cIBR7 using HL-60 Cells

To evaluate whether cIBR7 can be internalized via a receptor-mediated pathway, FITC-cIBR7 was synthesized and evaluated for its internalization properties in a temperature-dependent manner using confocal microscopy. FITC-dextran was used as a positive control because it is known to enter cells by fluid phase non-specific endocytosis.²¹ When incubated at 37 °C for 1 h, FITC-cIBR7 localized inside the HL-60 cells in the form of punctate stains (Figure 5a), suggesting that it was located in the endocytic compartments. It did not show a diffuse cytoplasmic distribution pattern as did the DOX-peptide conjugates. FITC-dextran also showed endosomal punctate localization after incubation at 37 °C (Figure 5c). When the temperature was reduced to 4 °C, no fluorescence associated with cells incubated with FITC-cIBR7 (Figure 5b) or FITC-dextran (Figure 5d) was observed. Thus, lowering the temperature to 4 °C knocks out the endocytic uptake pathway. These results suggested that FITC-cIBR7 entry into the HL-60 cells took place via the endocytic uptake pathway and that this entry was energy dependent.

Colocalization Studies of FITC-cIBR and FITC-cIBR7 with Alexa 647-Dextran using HL-60 Cells

To understand the intracellular distribution and destination of the conjugates, cells were incubated with Alexa 647-dextran and either FITC-cIBR or FITC-cIBR7 and were evaluated using confocal microscopy. The excitation and emission maxima for FITC are at 494 nm and 521 nm, respectively, while the excitation and emission maxima for Alexa 647 are at 650 nm and 668 nm, respectively. Alexa 647-dextran was used to avoid the artifacts of bleed-through or crossover of the fluorescence emission. The endocytosis of the dextran molecules is via a non-specific, fluid-phase endocytic pathway, and these molecules move gradually through the early endosomes, the late endosomes and finally into the lysosomes after entering the cells.²¹ Therefore, colocalization of the FITC-labeled peptides with dextran molecules would indicate that the FITC-labeled peptides followed a pathway similar to that of dextran into the lysosomes. The results showed that FITC-cIBR did not completely colocalize with dextran molecules after incubation for 1 h (Figure 6). Although there was a general trend of localization of FITC-cIBR and dextran molecules in the similar areas of the individual cells, they did not completely superimpose. Variations in the uptake of these two molecules can be observed and are a possible reason for this different distribution (Figures 6a, b). It may also suggest localization of some fractions of the peptide in other cellular compartments. The distribution profile of FITC-cIBR7 with dextran molecules was similar to that between FITC-cIBR and dextran (Figure 7). These observations suggested that both FITC-cIBR and FITC-cIBR7 might follow a pathway different from that of dextran inside the cell. It may also indicate that 1-h time period was not long enough to allow the molecules to reach their intracellular destination.

Discussion

Previously, we have shown that FITC-cIBR conjugate enters the HL-60 and Molt-3 cells via an energy-dependent pathway because its uptake is inhibited by ATP inhibitors such as sodium azide and 2-deoxy-D-glucose.¹⁴ LFA-1-deficient HUVEC also did not internalize the FITC-cIBR conjugate; in contrast, HUVEC internalized FITC-dextran. FITC-cIBR and FITC-dextran have a different cell entry profile when incubated with ATP inhibitors. The cells

incubated with ATP inhibitors showed punctate stains around the cells when treated with FITC-cIBR but the FITC-dextran-treated cells did not have any punctuated stains, suggesting FITC-cIBR binds to the cell surface receptor such as LFA-1. In addition, FITC-cIBR colocalizes with anti-LFA-1 antibody on MOLT-3 T-cells, indicating that it binds to the I-domain of LFA-1.²² Recently, cIBR peptide was shown (by antibody inhibition and NMR studies) to bind to the I-domain of LFA-1.^{23,24} Using mutation studies, smaller linear and cyclic derivatives of cIBR peptide (*i.e.*, cIBR7) have been found to have similar or better activity than the parent cIBR to inhibit ICAM-1/LFA-1-mediated heterotypic T-cell adhesion.^{18,25} During these studies, we found that cIBR7 cyclic peptide has better activity than cIBR to inhibit heterotypic T-cell adhesion, and the binding affinity of cIBR7 to the isolated I-domain is higher than that of cIBR peptide. However, the internalization properties of cIBR7 have not yet been elucidated.

Mutation and alanine-scanning studies indicated that the recognition sequence in cIBR peptide is at the Pro-Arg-Gly-Gly (PRGG)²⁵ and this sequence is in a β -turn conformation as determined by NMR studies.²⁶ The importance of the “PRGG” sequence and its β -turn conformation was further demonstrated by the efficiency of linear hexapeptide LH7 (PRGGSV) in inhibiting heterotypic T-cell adhesion to Caco-2 monolayers. LH7 peptide was cyclized (to generate CH7) using the N- and C- termini, which resulted in stabilization of the β -turn structure at the PRGG sequence. However, N- to C-terminal conjugation did not leave any suitable chemical functionality in the peptide for conjugation with drugs. In addition, introduction of Lys⁵ in place of Ser⁵ to give cyclo(1,6)PRGGKV for providing a drug conjugation site resulted in lower peptide activity.²⁵ Therefore, the cyclization method was altered by using a disulfide bond to produce cIBR7 (cyclo(1,8)CPRGGVC), which has free N- and C-termini that can be conjugated to drugs. As mentioned previously, this peptide has better binding properties to LFA-1 than does the parent cIBR. In addition, due to the removal of the C-terminal hydrophobic residues (LVTG sequence) from the parent cIBR peptide, cIBR7 is more hydrophilic than cIBR and offers an attractive opportunity to explore the influence of the physicochemical properties on the internalization of the DOX-peptide conjugates.

To evaluate the effect of conjugate hydrophilicity on their uptake properties, we have synthesized DOX-cIBR7, DOX-PEGcIBR7, and DOX-cIBR (Figure 1). DOX-cIBR7 conjugate was, indeed, more hydrophilic than DOX-cIBR (Table 1). Addition of a more hydrophilic linker in DOX-PEGcIBR7 produced a conjugate that was more hydrophilic than DOX-cIBR7. Unfortunately, both DOX-cIBR7 and DOX-PEGcIBR7 conjugates entered the HL-60 cells by an energy-independent pathway. Reduction of the temperature from 37 °C to 4 °C failed to inhibit the entry of the conjugates inside the cells. In addition, the distribution profile of the conjugates inside the cell cytosol was indicative of the non-endocytic uptake pathway. The conjugates did not show localization into distinct endocytic compartments. These results indicated that the change in hydrophobicity of the DOX-peptide conjugates does not influence their internalization behavior.

There are several possible explanations for the internalization behavior of the DOX-peptide conjugates. First, there is a possibility that the DOX segment of the conjugate interacts with the DOX segments of other molecules via anthraquinone stacking to form aggregates. These aggregates could readily partition into the lipid bilayer in spite of the presence of the targeting peptide. Second, the formation of aggregates can impose steric hindrance to the recognition site of the peptide by the LFA-1 receptors on the cell surface. Third, the DOX-segment of the conjugate has a high affinity for the membrane components, which would make it difficult for the remaining part of the conjugate (*i.e.*, peptide portion) to bind to LFA-1 and control the internalization process of the conjugate.

Aggregation of DOX molecules in aqueous solution has been observed and was proposed as the reason for the saturation kinetics and temperature-dependent entry of DOX into human red

blood cells. At normal physiological pH and temperature, DOX molecules exist in both neutral and charged forms; however, only the neutral form partitions into the cell membrane. Random association of the molecules through hydrophobic interactions leads to the formation of aggregates with associated charges. Only the uncharged monomer form can permeate the cell. Reduction of temperature leads to lower permeation into the cell as it increases aggregation because of lower Brownian motion.²⁰ Similarly, dimer and tetramer formation for DOX and daunorubicin (DNR) in aqueous solution have also been reported. These aggregation reactions take place through self-association of the planar aromatic ring systems.²⁷ DNR molecules were found to dimerize below 50 nM concentration; at higher concentration the dimers were proposed to self associate leading to a much more complex association scheme.²⁸ The possibility of transporter-mediated uptake for DOX has also been suggested.²⁹ Structural modification of anthracycline antibiotics produced tremendously different cellular entry behavior into Ehrlich ascites tumor cells. DOX, DNR, and rubidazole (RBD) showed a saturable, biphasic uptake pattern into these cell lines, with the initial rate of uptake being influenced by the structural modifications. DOX, DNR, and RBD showed temperature-dependent uptake. Moreover, unlabeled DNR inhibited the uptake of [³H]-DNR into these cells. All these properties are characteristic of transporter-mediated uptake.²⁹ Although there is no proof of any carrier-mediated transport for DOX in HL-60 cells, this idea, in addition to passive diffusion, may still be plausible for the uptake of DOX. It is not surprising that DOX and DNR have high affinity toward the cell membrane as there are membrane proteins with aromatic amino acids that can form molecular associations with the drug molecules through pi-electron interaction.

The aromatic doxomycinone moiety in DOX is responsible for its hydrophobic nature.¹³ Similar to DOX-cIBR, conjugates of DOX with other peptides could have higher hydrophobicity than DOX itself.¹⁰ For example, DOX-CNGRC conjugate was internalized to a similar extent into the cells with different levels of expression of the target receptor, indicating that this conjugate was not internalized via a receptor-mediated pathway.¹⁰ DOX-cIBR also entered the HL-60 cells in the absence of energy-dependent mechanism and showed diffuse cytoplasmic distribution. Hydrophobicity of the DOX-cIBR conjugate was proposed to be the reason for its energy-independent cytosolic entry into the HL-60 cells. A similar hypothesis was proposed for the cytosolic, non-specific entry of DOX-CNGRC conjugate into the cells.¹⁰ Our previous¹⁴ and present studies clearly demonstrate that the hydrophobicity of the DOX-peptide conjugates is not the only factor in determining their internalization behavior. The distribution ratio for DOX-CNGRC (5.3, pH 7.4) is similar to that of our DOX-cIBR7 (distribution ratio 4.3, pH 7.4). DOX-PEGcIBR7 has a distribution ratio of 0.9 at pH 7.4, which is comparable to that of DOX (distribution ratio 1.2, pH 7.4^{10,14}). However, DOX-PEGcIBR7 has internalization properties similar to those of the other DOX conjugates. These results suggest that the entry of DOX-peptide conjugates may not be influenced by hydrophobicity or the targeting moiety of the conjugate, but may be driven by the physical properties of the DOX fragment of the conjugate. Although there are several proposals on how DOX enters the cells, there have been no systematic studies to elucidate the mechanism(s) of DOX entry into the cells.

The hypothesis that the discrepancy in the internalization behavior of the DOX-peptide conjugates was due to the properties of the DOX molecule or the final conjugate was demonstrated by the energy-dependent uptake of FITC-cIBR7 peptide. If this were due to the properties of cIBR7 peptide, FITC-cIBR7 would also show energy-independent internalization properties. However, FITC-cIBR7 showed a temperature-dependent endocytic entry into the HL-60 cells similar to that of FITC-cIBR.¹⁴ Similarly, FITC-labeled transferrin protein showed energy-dependent uptake into L929 cells, whereas the DOX-conjugate of transferrin protein (TRF-DOX) showed energy-independent cellular entry into the same cells. In addition, the uptake of the TRF-DOX conjugate could not be blocked by excess TRF.⁸

Colocalization studies of both FITC-cIBR and FITC-cIBR7 with dextran molecules suggested the different cellular localization of the peptides compared to the dextran molecules. After their endocytic entry, these peptides might take a different route inside the cells compared to dextran. It is also possible that the peptides were captured on the way to their final intracellular destination. The target receptor (LFA-1) for these peptides was shown to undergo caveolin-mediated endocytosis. In human polymorphonuclear neutrophils, the LFA-1 receptor did not colocalize with LAMP-1 (a marker for late endosome or lysosome). In CHO cell, LFA-1 never colocalized with clathrin-coated pits.³⁰ Molecules internalized by the clathrin coat mediated pathway are often finally localized in the cellular lysosomes. Molecules internalized by caveolin-mediated endocytosis are also known to be finally localized in the cellular Golgi compartment.³¹ All of these observations suggested that cIBR7 peptide, like cIBR peptide, has the potential to target drugs to leukocytes. Identification of the possible digestion product of the FITC-labeled peptides will help in designing a specific conjugation approach to release the free drug for interaction with intracellular targets. As an alternative method to deliver DOX, this drug can be encapsulated in nanoparticles or liposomes that are decorated with targeting peptides to avoid non-specific delivery of DOX as shown above. The objective would be to prevent the formation of DOX aggregates followed by direct interaction of DOX and its aggregates with cell membranes. Decorating the surfaces of nanoparticles with cIBR or cIBR7 peptide may allow internalization of these carriers by LFA-1-expressing leukocytes to carry the loaded drugs into the cells.

Conclusions

In conclusion, we have shown that internalization of DOX-peptide conjugates is not influenced by the physicochemical properties of the conjugate. Irrespective of the size or hydrophobicity of the conjugates, they retain the energy-independent cellular entry. Unlike DOX-cIBR7 conjugates, the FITC-cIBR7 peptides showed energy-dependent cellular entry into the cells, suggesting that these two conjugates have different internalization mechanisms. The FITC-labeled peptides showed different intracellular distribution compared to dextran molecules inside the cells. Although DOX is a highly effective anticancer agent, this molecule presents a unique challenge for targeted drug delivery. Currently, we are conjugating cIBR7 peptide with anticancer drugs having different physicochemical properties (*i.e.*, hydrophilicity) for selective delivery to leukemic cells. The hope is that the drug-cIBR/cIBR7 conjugate will enter via LFA-1-mediated endocytosis similar to the entry of FITC-cIBR/cIBR7.

Acknowledgements

This work is supported by the National Institutes of Health (R01-AI-063002). We would like to thank Merck Inc. and Amgen Inc. Predoctoral Fellowships to SM. We also thank Nancy Harmony for proofreading the manuscript.

References

1. Nagy A, Armatis P, Cai RZ, Szepeshazi K, Halmos G, Schally AV. Design, Synthesis, and in Vitro Evaluation of Cytotoxic Analogs of Bombesin-Like Peptides Containing Doxorubicin or Its Intensely Potent Derivative, 2-Pyrrolinodoxorubicin. *Proc Natl Acad Sci USA* 1997;94:652–656. [PubMed: 9012839]
2. Nagy A, Schally AV, Armatis P, Szepeshazi K, Halmos G, Kovacs M, Zarandi M, Groot K, Miyazaki M, Jungwirth A, Horvath J. Cytotoxic Analogs of Luteinizing Hormone-Releasing Hormone Containing Doxorubicin or 2-Pyrrolinodoxorubicin, a Derivative 500–1000 Times More potent. *Proc Natl Acad Sci USA* 1996;93:7269–7273. [PubMed: 8692981]
3. Nagy A, Schally AV, Halmos G, Armatis P, Cai RZ, Csernus V, Kovacs M, Koppan M, Szepeshazi K, Kahan Z. Synthesis and Biological Evaluation of Cytotoxic Analogs of Somatostatin Containing Doxorubicin or Its Intensely Potent Derivative, 2-Pyrrolinodoxorubicin. *Proc Natl Acad Sci USA* 1998;95:1794–1799. [PubMed: 9465096]

4. Anderson ME, Siahaan TJ. Targeting Icam-1/Lfa-1 Interaction for Controlling Autoimmune Diseases: Designing Peptide and Small Molecule Inhibitors. *Peptides* 2003;24:487–501. [PubMed: 12732350]
5. Duneahoo AL, Anderson ME, Majumdar S, Kobayashi N, Berkland C, Siahaan TJ. Cell Adhesion Molecules for Targeted Drug Delivery. *J Pharm Sci* 2006;95:1856–1872. [PubMed: 16850395]
6. Nagy A, Schally AV. Targeting Cytotoxic Conjugates of Somatostatin, Luteinizing Hormone-Releasing Hormone and Bombesin to Cancers Expressing Their Receptors: A “Smarter” Chemotherapy. *Curr Pharm Design* 2005;11:1167–1180.
7. Lu Y, Yang J, Sega E. Issues Related to Targeted Delivery of Proteins and Peptides. *AAPS J* 2006;8:E466–478. [PubMed: 17025264]
8. Lai BT, Gao JP, Lanks KW. Mechanism of Action and Spectrum of Cell Lines Sensitive to a Doxorubicin-Transferrin Conjugate. *Cancer Chemother Pharmacol* 1998;41:155–160. [PubMed: 9443629]
9. Garnett MC. Targeted Drug Conjugates: Principles and Progress. *Adv Drug Deliv Rev* 2001;53:171–216. [PubMed: 11731026]
10. van Hensbergen Y, Broxterman HJ, Elderkamp YW, Lankelma J, Beers JC, Heijn M, Boven E, Hoekman K, Pinedo HM. A Doxorubicin-Cnrgc-Peptide Conjugate with Prodrug Properties. *Biochem Pharmacol* 2002;63:897–908. [PubMed: 11911842]
11. Kratz F, Beyer U, Roth T, Tarasova N, Collery P, Lechenault F, Cazabat A, Schumacher P, Unger C, Falken U. Transferrin Conjugates of Doxorubicin: Synthesis, Characterization, Cellular Uptake, and in Vitro Efficacy. *J Pharm Sci* 1998;87:338–346. [PubMed: 9523988]
12. Froesch BA, Stahel RA, Zangemeister-Wittke U. Preparation and Functional Evaluation of New Doxorubicin Immunoconjugates Containing an Acid-Sensitive Linker on Small-Cell Lung Cancer Cells. *Cancer Immunol Immunother* 1996;42:55–63. [PubMed: 8625367]
13. Chaires JB, Satyanarayana S, Suh D, Fokt I, Przewloka T, Priebe W. Parsing the Free Energy of Anthracycline Antibiotic Binding to DNA. *Biochem* 1996;35:2047–2053. [PubMed: 8652545]
14. Majumdar S, Kobayashi N, Krise JP, Siahaan TJ. Mechanism of Internalization of an Icam-1-Derived Peptide by Human Leukemic Cell Line HI-60: Influence of Physicochemical Properties on Targeted Drug Delivery. *Mol Pharm* 2007;4:749–758. [PubMed: 17680719]
15. Kruger M, Beyer U, Schumacher P, Unger C, Zahn H, Kratz F. Synthesis and Stability of Four Maleimide Derivatives of the Anticancer Drug Doxorubicin for the Preparation of Chemoimmunoconjugates. *Chem Pharm Bull* 1997;45:399–401.
16. Garsky VM, Lumma PK, Feng DM, Wai J, Ramjit HG, Sardana MK, Oliff A, Jones RE, DeFeo-Jones D, Freidinger RM. The Synthesis of a Prodrug of Doxorubicin Designed to Provide Reduced Systemic Toxicity and Greater Target Efficacy. *J Med Chem* 2001;44:4216–4224. [PubMed: 11708923]
17. Denmeade SR, Nagy A, Gao J, Lilja H, Schally AV, Isaacs JT. Enzymatic Activation of a Doxorubicin-Peptide Prodrug by Prostate-Specific Antigen. *Cancer Res* 1998;58:2537–2540. [PubMed: 9635575]
18. Iskandarsyah; Tejo BA, Tambunan US, Verkhivker G, Siahaan TJ. Structural Modifications of Icam-1 Cyclic Peptides to Improve the Activity to Inhibit Heterotypic Adhesion of T Cells. *Chem Biol Drug Des* 2008;72:27–33. [PubMed: 18554252]
19. Gursoy RN, Siahaan TJ. Binding and Internalization of an Icam-1 Peptide by the Surface Receptors of T Cells. *J Pept Res* 1999;53:414–421. [PubMed: 10406219]
20. Dalmark M, Storm HH. A Fickian Diffusion Transport Process with Features of Transport Catalysis. Doxorubicin Transport in Human Red Blood Cells. *Journal of General Physiology* 1981;78:349–364. [PubMed: 7288392]
21. Baravalle G, Schober D, Huber M, Bayer N, Murphy RF, Fuchs R. Transferrin Recycling and Dextran Transport to Lysosomes Is Differentially Affected by Bafilomycin, Nocodazole, and Low Temperature. *Cell Tissue Res* 2005;320:99–113. [PubMed: 15714281]
22. Anderson ME, Siahaan TJ. Mechanism of Binding and Internalization of Icam-1-Derived Cyclic Peptides by Lfa-1 on the Surface of T Cells: A Potential Method for Targeted Drug Delivery. *Pharm Res* 2003;20:1523–1532. [PubMed: 14620502]
23. Anderson ME, Tejo BA, Yakovleva T, Siahaan TJ. Characterization of Binding Properties of Icam-1 Peptides to Lfa-1: Inhibitors of T-Cell Adhesion. *Chem Biol Drug Design* 2006;68:20–28.

24. Zimmerman T, Oyarzabal J, Sebastian ES, Majumdar S, Tejo BA, Siahaan TJ, Blanco FJ. Icam-1 Peptide Inhibitors of T-Cell Adhesion Bind to the Allosteric Site of Lfa-1. An Nmr Characterization. *Chem Biol Drug Design* 2007;70:347–353.
25. Anderson ME, Yakovleva T, Hu Y, Siahaan TJ. Inhibition of Icam-1/Lfa-1-Mediated Heterotypic T-Cell Adhesion to Epithelial Cells: Design of Icam-1 Cyclic Peptides. *Bioorg Med Chem Lett* 2004;14:1399–1402. [PubMed: 15006370]
26. Gursoy RN, Jois DS, Siahaan TJ. Structural Recognition of an Icam-1 Peptide by Its Receptor on the Surface of T Cells: Conformational Studies of Cyclo (1, 12)-Pen-Pro-Arg-Gly-Gly-Ser-Val-Leu-Val-Thr-Gly-Cys-OH. *J Pept Res* 1999;53:422–431. [PubMed: 10406220]
27. Eksborg S. Extraction of Daunorubicin and Doxorubicin and Their Hydroxyl Metabolites: Self-Association in Aqueous Solution. *J Pharm Sci* 1978;67:782–785. [PubMed: 660455]
28. Barthelemy-Clavey V, Maurizot JC, Dimicoli JL, Sicard P. Self-Association of Daunorubicin. *FEBS Lett* 1974;46:5–10. [PubMed: 4417418]
29. Skovsgaard T. Carrier-Mediated Transport of Daunorubicin, Adriamycin, and Rubidazone in Ehrlich Ascites Tumour Cells. *Biochem Pharmacol* 1978;27:1221–1227. [PubMed: 567991]
30. Fabbri M, Di Meglio S, Gagliani MC, Consonni E, Molteni R, Bender JR, Tacchetti C, Pardi R. Dynamic Partitioning into Lipid Rafts Controls the Endo-Exocytic Cycle of the Alpha/Beta2 Integrin, Lfa-1, During Leukocyte Chemotaxis. *Mol Biol Cell* 2005;16:5793–5803. [PubMed: 16207819]
31. Razani B, Lisanti MP. Caveolins and Caveolae: Molecular and Functional Relationships. *Exp Cell Res* 2001;271:36–44. [PubMed: 11697880]

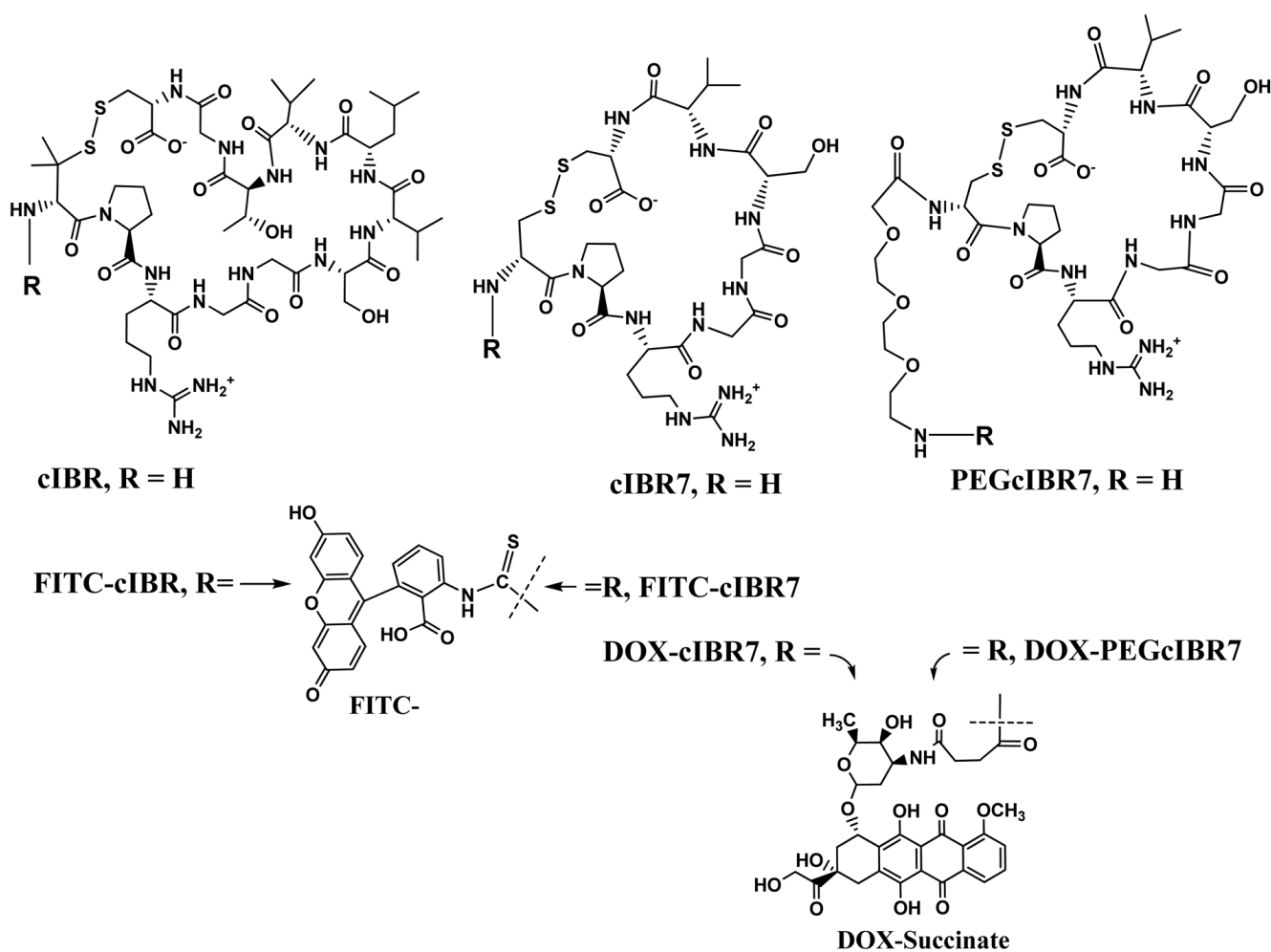


Figure 1.

The chemical structures of cIBR peptide (cyclo(1,12)PenPRGGSVLVTGC) and its derivatives cIBR7 (cyclo(1,8)CPRGGSVC) and PEGcIBR7 (PEG-cyclo(1,8)CPRGGSVC). These peptides were conjugated to the carboxylic acid of DOX-succinate from their free N-terminus. cIBR7 peptide was synthesized by removing the LVTG sequence from the C-terminal of cIBR peptide. Pen1 in cIBR was replaced by Cys1 in cIBR7. PEGcIBR7 peptide was synthesized by conjugating 11-amino-3,6,9-trioxaundecanoic acid to the N-terminal of the cIBR7 peptide.

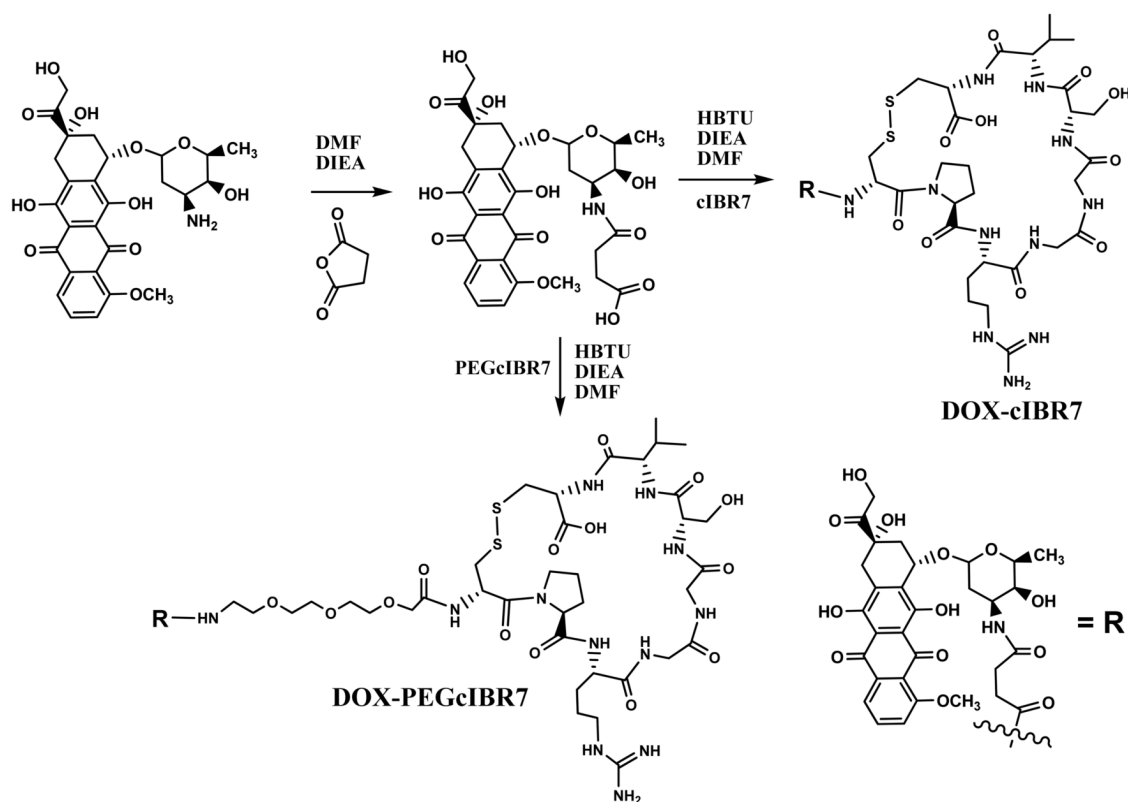


Figure 2. Synthesis of DOX conjugates of cIBR7 and PEGcIBR7 peptides to produce DOX-cIBR7 and DOX-PEGcIBR7 conjugates. Primary amine of the daunosamine of DOX was derivatized using succinic anhydride to generate DOX-succinate. The N-terminal of the peptides was conjugated to the carboxylic acid group of DOX-succinate via an amide bond.

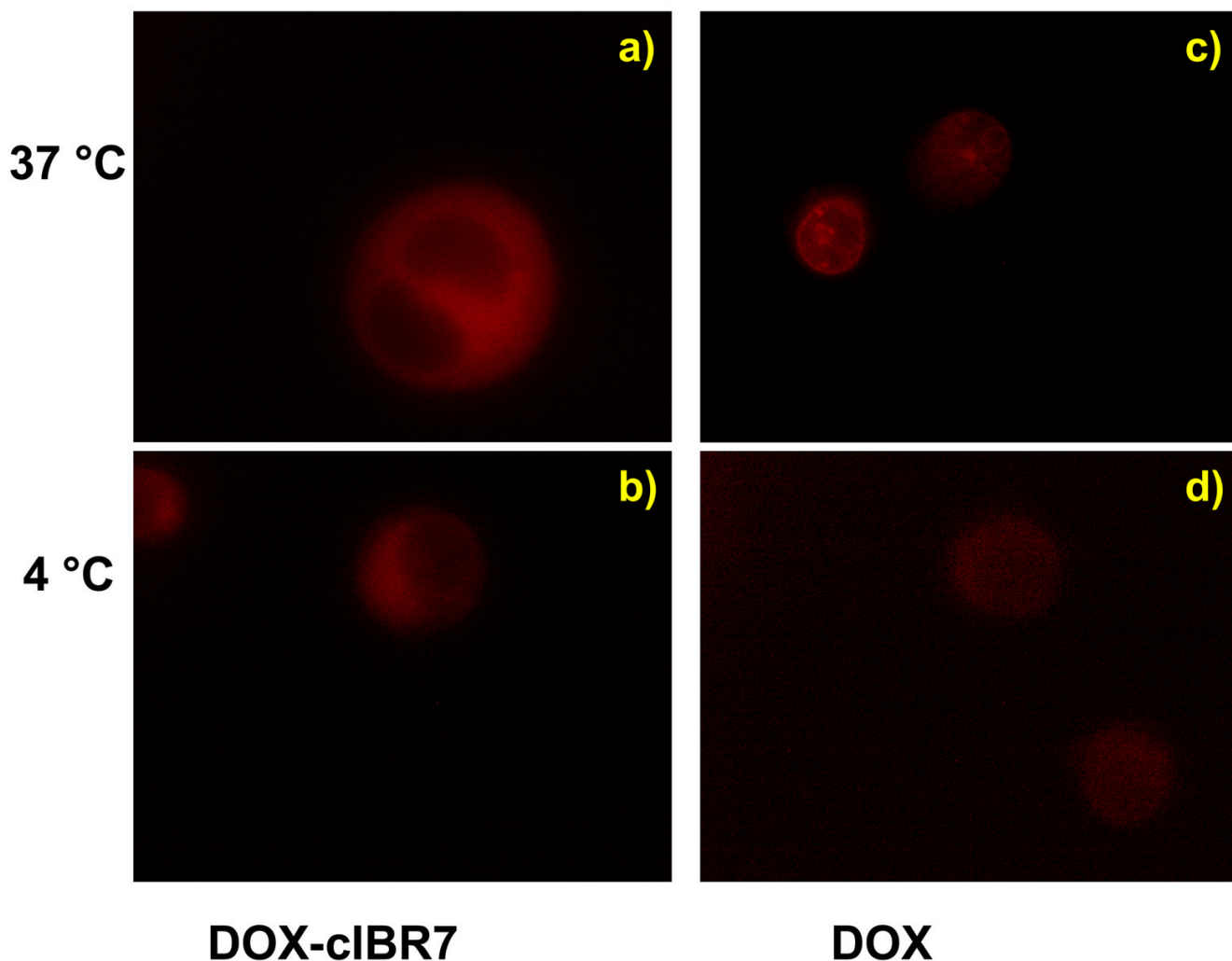


Figure 3. DOX-cIBR7 conjugate entry into the HL-60 cells was not affected by change in temperature as evaluated by an epifluorescence microscope. Panel **a)** illustrates that DOX-cIBR7 showed diffuse fluorescence distribution in the cell cytoplasm after incubation at 37 °C. It did not show the punctate intracellular stain indicative of endocytosis. Panel **b)** demonstrates that incubation at 4 °C did not inhibit the conjugate entry or change the distribution pattern. For comparison, profiles of the cells incubated with DOX at 37 °C and 4 °C are shown in panels **c)** and **d)**, respectively.

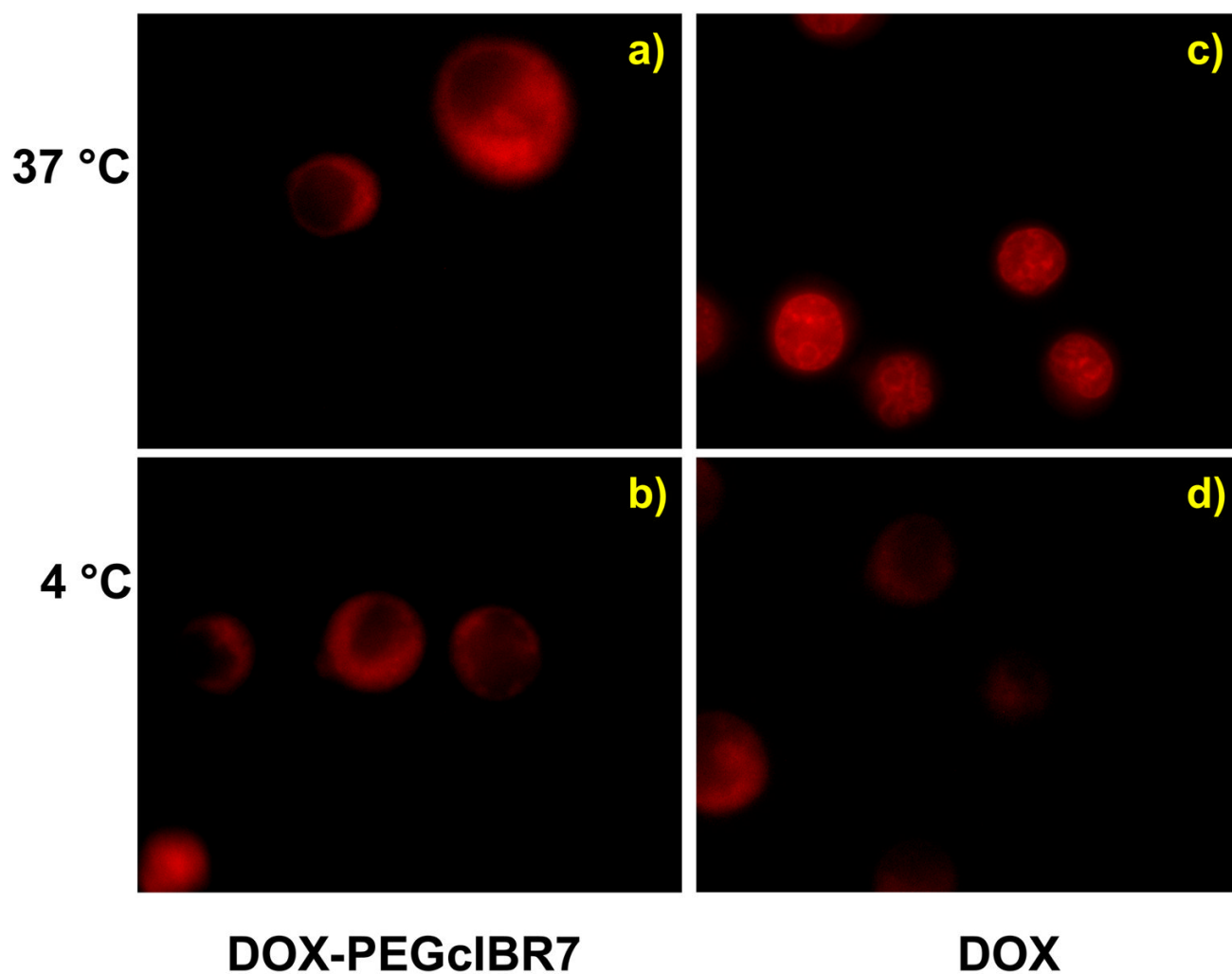


Figure 4. An increase in hydrophilicity of the DOX-PEGcIBR7 conjugate did not change the cellular entry mechanism or the distribution pattern compared to DOX-cIBR7 in HL-60 cells evaluated by epifluorescence microscope. Panel **a)** shows cells incubated with DOX-PEGcIBR7 at 37 °C. Panel **b)** shows cells incubated with DOX-PEGcIBR7 at 4 °C. Under both conditions, the conjugate showed diffuse cytoplasmic fluorescence distribution patterns. Profiles of the cells incubated with DOX at 37 °C and 4 °C are shown in panels **c)** and **d)**, respectively.

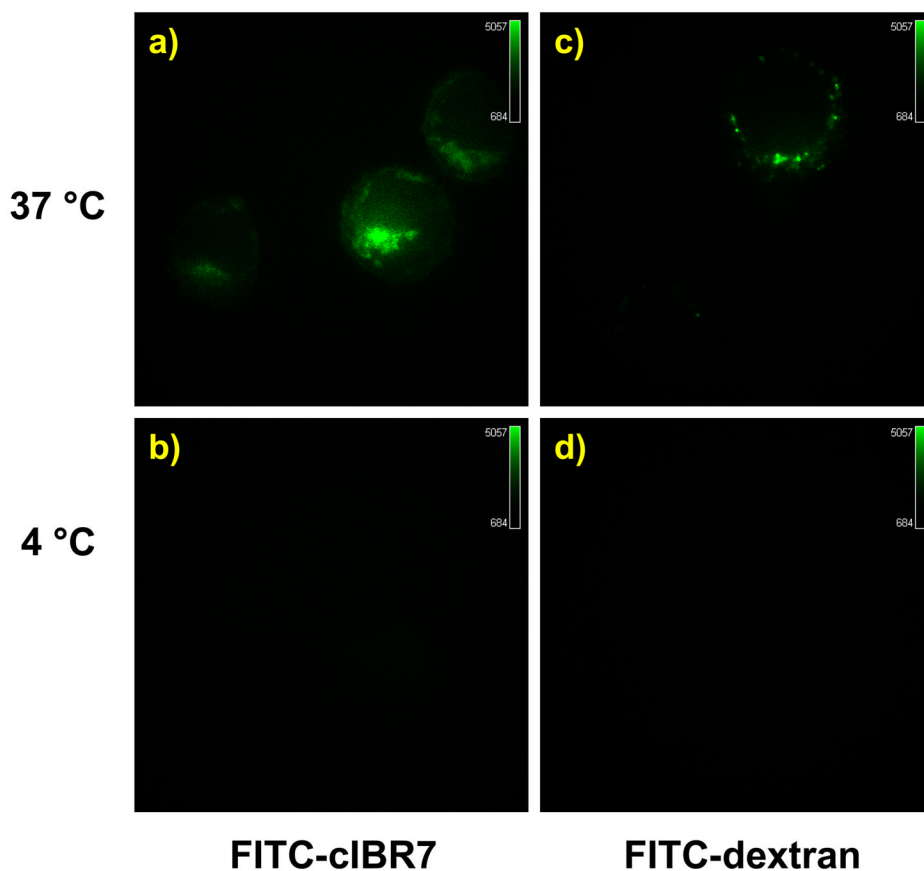


Figure 5. FITC-cIBR7 showed temperature-dependent internalization in HL-60 cells evaluated using a confocal microscope. Panel **a**) shows cells incubated with FITC-cIBR7 at 37 °C. Distinct localization of FITC-cIBR7 is indicative of an endocytic uptake pathway. **b**) Incubation of the cells at 4 °C prevented the endocytic uptake of FITC-cIBR7, suggesting that the entry was energy-dependent. As a control, FITC-dextran internalization profiles at 37 °C and 4 °C are shown in panels **c**) and **d**), respectively.

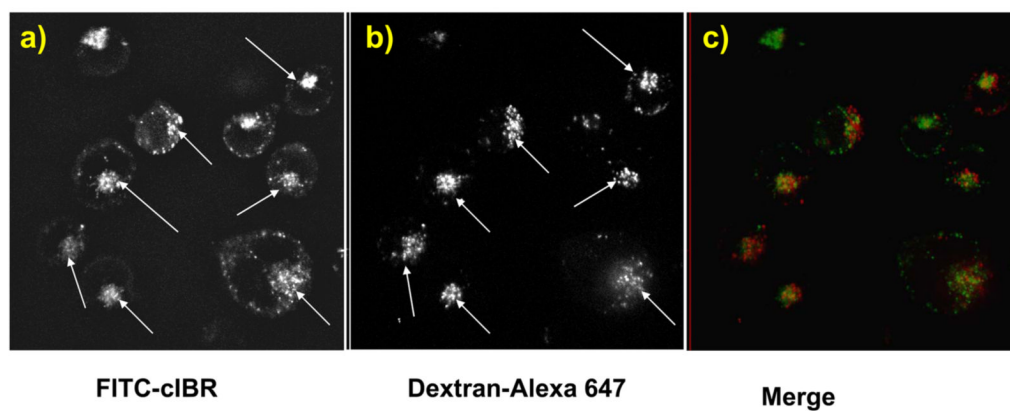


Figure 6. Intracellular distribution study of FITC-cIBR and Alexa 647-labeled dextran molecules after incubation for 1 h with HL-60 cells evaluated using a confocal microscope. Panel **a)** shows the intracellular distribution for FITC-cIBR. Panel **b)** shows the localization of the Alexa 647-labeled dextran under the same conditions. Panel **c)** is a merger of panels **a)** and **b)**.

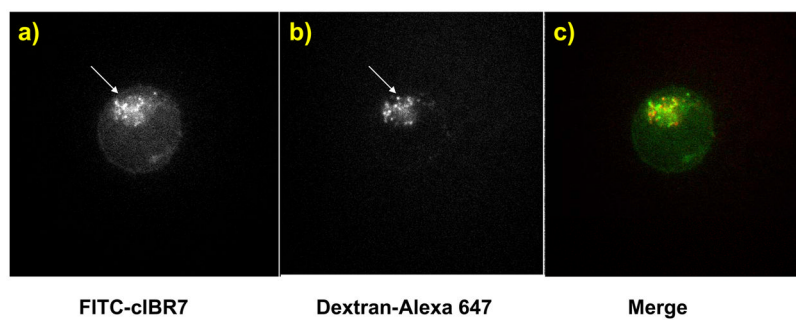


Figure 7. Intracellular distribution study of FITC-cIBR7 and Alexa 647-labeled dextran molecules after incubation for 1 h with HL-60 cells evaluated with a confocal microscope. Panel a) shows the intracellular distribution for FITC-cIBR7. Panel b) shows the localization of Alexa 647-labeled dextran under the same conditions. Panel c) is a merger of panels a) and b).

Table 1

Octanol/aqueous buffer (pH 7.4) distribution ratios for DOX-cIBR7 and DOX-PEGcIBR7 and comparison with DOX-cIBR (from Majumdar *et al.*¹⁴)

Compound	Distribution Ratio (D)	Log D
DOX-cIBR7	4.3	0.63
DOX-PEGcIBR7	0.9	-0.04
DOX-cIBR	14.1	1.14